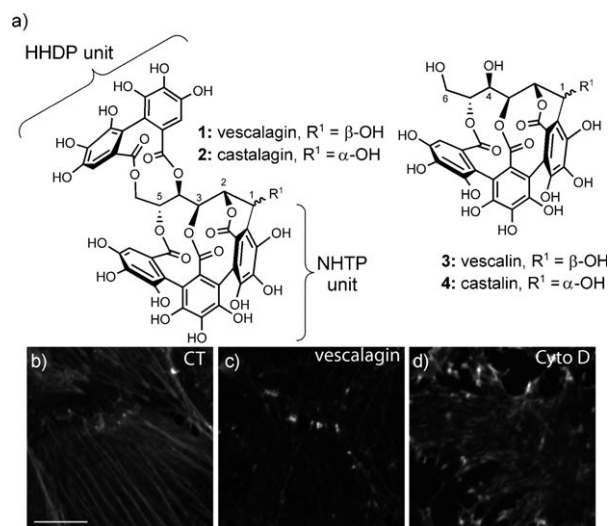


# Binding of Filamentous Actin and Winding into Fibrillar Aggregates by the Polyphenolic C-Glucosidic Ellagitannin Vescalagin\*\*

Stéphane Quideau,\* Céline Douat-Casassus, Daniela Melanè Delannoy López, Carmelo Di Primo, Stefan Chassaing, Rémi Jacquet, Frédéric Saltel, and Elisabeth Genot\*

Herein we describe the effects of the C-glucosidic ellagitannin vescalagin (**1**, Figure 1 a), a polyphenolic natural product readily available from fagaceous woody plant sources, such as oak (*Quercus* sp.),<sup>[1]</sup> on actin, one of the most abundant structural proteins in eukaryotic cells. Monomeric globular actin (G-actin) subunits assemble through an adenosine triphosphate (ATP) dependent process into polymeric fibrillar actin (F-actin) filaments, which are further ordered into three-dimensional architectures to establish the functional actin cytoskeleton.<sup>[2]</sup> A dynamic equilibrium between the G-actin and F-actin states continuously ensures the adaptation of the actin cytoskeleton during its various roles in controlling cell shape, cytokinesis, motility, adhesion, and gene expression.<sup>[3]</sup>

Natural products have been key players in probing the role of actin by perturbing the assembly and/or disassembly of actin filaments.<sup>[4]</sup> The bicyclic heptapeptide fungal metabolite phalloidin and the cyclodepsipeptide sponge or microbial metabolites jasplakinolide and chondramide C bind to F-actin and inhibit depolymerization by strengthening actin-actin



**Figure 1.** a) Structures of the four oak-derived C-glucosidic ellagitannins used in the antiactin in cellulo assay. b–d) Fluorescent images showing F-actin organization in untreated BAE cells (b), in BAE cells exposed to vescalagin (**1**, 50  $\mu\text{M}$ ) for 1 h (c), and in BAE cells exposed to cytochalasin D (4  $\mu\text{M}$ ) for 1 h (d). Scale bar: 5  $\mu\text{m}$ . CT = control.

[\*] Prof. S. Quideau, Dr. C. Douat-Casassus, D. M. Delannoy López, Dr. S. Chassaing, R. Jacquet  
 Université de Bordeaux  
 Institut des Sciences Moléculaires (CNRS-UMR 5255)  
 Institut Européen de Chimie et Biologie (IECB)  
 2 rue Robert Escarpit, 33607 Pessac Cedex (France)  
 Fax: (+33) 5-4000-2215  
 E-mail: s.quideau@iecb.u-bordeaux.fr

Dr. C. Di Primo  
 IECB/INSERM U869  
 2 rue Robert Escarpit, 33607 Pessac Cedex (France)

Dr. F. Saltel,<sup>[†]</sup> Dr. E. Genot<sup>[†]</sup>  
 IECB/INSERM U1053  
 2 rue Robert Escarpit, 33607 Pessac Cedex (France)  
 Fax: (+33) 5-4000-3076  
 E-mail: e.genot@iecb.u-bordeaux.fr

[†] These authors contributed equally.

[\*\*] Financial support from the Agence Nationale de la Recherche (ANR-06-BLAN-0139 and ANR-06-BLAN-0362), the Conseil Régional d'Aquitaine (grant 20071301020), La Ligue Contre le Cancer (Comité Dordogne 2006 and 2007), and the Institut Européen de Chimie et Biologie (2007 Internal Seed Grant Program) is gratefully acknowledged. D.M.D.L. acknowledges the support of Fundayacuco and the French Embassy in Caracas, Venezuela, for her doctoral research assistantship. We thank A. Nube, A. Labrousse, and I. Maridonneau-Parini for preliminary experiments, R. Boujema-Paterski and L. Blanchoin for reagents and precious advice on actin polymerization assays, and A. Grelard for NMR spectroscopic experiments.



Supporting information for this article is available on the WWW under <http://dx.doi.org/10.1002/anie.201006712>.

interactions, whereas the marine macrolides known as latrunculins bind to G-actin and prevent actin-filament formation.<sup>[5]</sup> Other polyketide-derived natural products, such as the fungal metabolites named cytochalasins, bind to F-actin (and to G-actin) and thereby block both the assembly and disassembly of individual actin monomers.<sup>[5a]</sup> Herein we report that the polyphenolic plant metabolite vescalagin (**1**) not only interacts with actin filaments but also winds them into fibrillar aggregates in vitro and in cellulo.

Vescalagin (**1**) belongs to a particular group of ellagitannins<sup>[6]</sup> that comprises a unique series of highly hydrosoluble C-glucosidic variants. In these compounds, the usual ellagitannin glucopyranose core is replaced by an open-chain glucose moiety, which is rarely encountered in nature and results from the establishment of a C-aryl glucosidic bond.<sup>[7]</sup> Our interest in studying these C-glucosidic ellagitannins stems from the premise that the highly preorganized medium-sized-ring-containing multiple-phenol array featured by such natural products should be structurally well-suited to interfere with the construction of protein-made cellular architectures, such as actin filaments or microtubules.<sup>[5b]</sup> Some ellagitannins, which interfere with bone resorption, are known to affect osteoclastic actin rings.<sup>[8]</sup> We thus first examined the effect of a selection of four C-glucosidic ellagitannins on the actin cytoskeleton in living cells. These four compounds are the two

most abundant C-glucosidic ellagitannins found in oak heartwood, vescalagin (**1**) and its C1 epimer castalagin (**2**), and their two minor congeners, vescalin (**3**) and castalin (**4**), both of which lack the hexahydroxydiphenoyl (HHDP) unit at the 4- and 6-positions of the glucose core (Figure 1a).<sup>[1,9a]</sup>

We used bovine aortic endothelial (BAE) cells, a well-characterized type of primary cell.<sup>[10]</sup> Any of the four ellagitannins used at a concentration of 50  $\mu\text{M}$  rapidly provoked the disappearance of the internal stress-fiber network observed in control cells (see Figure 1b,c and Figure S1 in the Supporting Information). Cytochalasin D, known to inhibit F-actin polymerization,<sup>[5b,11]</sup> was also effective; however, the resulting actin perturbation appeared distinct from that induced by ellagitannins **1–4** (Figure 1d). Focal adhesions, which anchor stress fibers to the matrix through integrins,<sup>[12]</sup> underwent dissolution, suggestive of alterations in cell adhesion (see Figure S2). Overall, the changes in actin configuration elicited by **1–4** were markedly different from those induced by other natural products known to target actin.<sup>[5a,b]</sup> We focused thereafter on vescalagin (**1**), because it is the easiest of the four compounds to modify by selective chemical means,<sup>[9,13]</sup> and it is available in large quantities by extraction from its main natural sources.<sup>[9a]</sup>

The vescalagin-induced F-actin-disrupting effect seen in BAE cells was also observed in fibroblast cells (BHK-21), which also express  $\beta$ -actin as the main actin isoform, as well as in smooth muscle cells (A7r5), which, in contrast, predominantly express  $\alpha$ -actin (see Figure S3). Despite subtle differences, the impact of **1** on the actin cytoskeleton appeared neither cell- nor actin-isoform-specific, which suggests that **1** can affect all types of mammalian cells. Furthermore, like for cytochalasin D, no alteration of the microtubule network could be detected upon the treatment of cells with **1** (see Figure S4). Remarkably, all cytoskeletal alterations could be completely reversed within 1 hour by washing **1** from the cells with medium. Phenotype recovery occurred at a rate similar to that observed for cytochalasin D<sup>[14]</sup> (see Figure S5).

The vescalagin-induced dissolution of stress fibers affected cellular morphology and, eventually, viability. Within the range of concentrations and incubation times examined, cells changed their well-spread morphology to a more retracted morphology (see Movies 1–3 in the Supporting Information). Mitosis, still observed when **1** was used at a concentration of 50  $\mu\text{M}$  (see Movie 1), became impaired at 100  $\mu\text{M}$  (see Movie 2 and Figure S6). Staining with propidium iodide (PI) revealed no cytotoxicity after 24 hours at 50  $\mu\text{M}$ ; however, the presence of apoptotic nuclei, which indicate irreversible commitment to cell death, was eventually detected when cells were exposed to **1** at 100  $\mu\text{M}$ . Functional consequences for cells translated into impaired wound-repair capacity (see Figure S6). The efficient serum-induced stimulation of the healing of mechanically injured endothelium was decreased by about half in the presence of **1** at a concentration of 20  $\mu\text{M}$ . The denudated area remained virtually unpopulated for 6 hours after exposure to **1** at a concentration of 100  $\mu\text{M}$ ; these conditions are still compatible with the maintenance of cell viability (see Figure S6). These data illustrate the rapid (see Movies 1–3) and sustained effects of **1** on cells.

Live imaging carried out on BAE cells expressing actin-GFP and treated with **1** (100  $\mu\text{M}$ ) showed immediate alteration of actin-GFP distribution at cell margins (see Figure S7). Destabilization of the stress fibers was visualized by the progressive loss of filamentous staining (see Movie 4) concomitantly with cell retraction (see Movies 1–3). Noticeably, thick F-actin bundles were maintained. A fluorescence recovery after photobleaching (FRAP) assay on actin-GFP-expressing BAE cells in the absence or presence of **1** (Figure 2; see also Movies 5 and 6) revealed that **1** increases

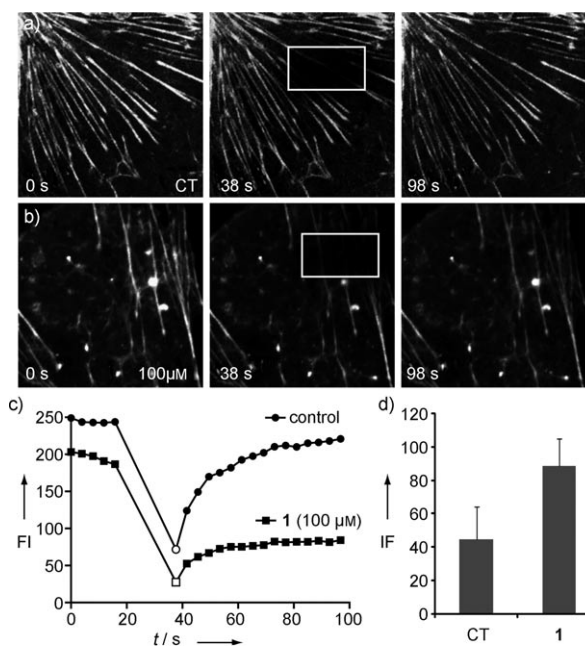


**Figure 2.** a,b) Live imaging of BAE cells expressing actin-GFP were subjected to FRAP in the absence (a) or presence (b) of vescalagin (**1**, 100  $\mu\text{M}$ ). The boxed region (200  $\times$  100 pixel square) was photobleached (before ( $t=0$  s), immediately after ( $t=38$  s), and after photobleaching ( $t=98$  s)). c) Normalized fluorescence intensity in the boxed region for the entire duration of the FRAP experiment. Fluorescence recovery (starting at the empty circle or square) recorded over time reveals the rates of actin turnover within this area. d) Quantitation of the results. The immobile fraction was calculated from the difference between the pre- and post-photobleaching intensities ( $n=6$ ). FI = fluorescence intensity; IF = immobile fraction.

the immobile fraction of actin trapped in F-actin bundles. We conclude that **1** affects both thin and thick actin fibers. However, thick F-actin bundles made of packed actin filaments are less vulnerable to the action of **1** than the single-filament dendritic meshwork at the cell periphery.

The rapidity with which **1** induces drastic perturbations within cells suggests that **1** is capable of crossing the plasma membrane. To investigate this behavior further, we prepared a fluorescent vescalagin derivative by chemical synthesis and tracked it in cellulose. After exploring various possibilities for the design of such a derivative with an appropriate fluorophore conveniently attached to the natural product, we settled on a vescalagin derivative equipped with a fluores-

cein-terminated 13-atom-long linker<sup>[15]</sup> by using fluorescein isothiocyanate (FITC) as the starting fluorophore. The choice of such a relatively long linker was made to prevent quenching of the fluorescein fluorescence through intramolecular interactions with the electronic-rich polyphenolic vescalagin-derived unit.<sup>[16]</sup> The synthesis of this vescalagin–FITC conjugate **6** commenced with the preparation of the fluorescein-terminated linker **5** on a solid support (see the Supporting Information for details). With this thiol-functionalized fluorescein derivative in hand, we took advantage of the known chemoselectivity expressed at the vescalagin hydroxylated C1 position under acid-catalyzed nucleophilic substitution reaction conditions<sup>[9,13]</sup> to forge the vescalagin–FITC conjugate **6** in 30% yield after purification by reversed-phase HPLC (Figure 3 a).

When added to living BAE cells, **6** displayed antiactin effects similar to those observed for **1** (Figure 1 c). This fluorescent vescalagin derivative colocalized with F-actin in the remaining internal thick stress fibers and aggregates (Figure 3 b); it was thus established that this compound had passed the plasma membrane and reached its target. To better visualize this target, we fixed the BAE cells to stabilize the actin cytoskeleton. After permeabilization, simultaneous staining with **6** and fluorescent Alexa546–phalloidin revealed that, in the absence of the actin-destabilization effect, **6**

highlighted the entire cytoskeleton (Figure 3 c), similarly to phalloidin; this result shows that **6** binds all actin fibers in cellulo.

To explore whether or not the interaction between vescalagin (**1**) and actin was direct, we set up an in vitro assay based on actin polymerization from a solution of Ca<sup>2+</sup>–actin–ATP monomers. Spontaneous polymerization occurred when Ca<sup>2+</sup> was replaced by the Mg<sup>2+</sup> ions present in the F-actin buffer.<sup>[17a]</sup> High-speed centrifugation of the samples enabled separation of the neoformed polymers from the monomers to discriminate the binding of **1** to either F-actin or G-actin, or both. To visualize these presumptive molecular associations, we again used the vescalagin fluorophore **6** and a fluorescent Alexa633–phalloidin conjugate to stain F-actin. Actin polymerization was allowed to reach the steady state under permissive and nonpermissive conditions (i.e., in the presence or absence of Mg<sup>2+</sup>-containing F-actin buffer) and was continued for 30 min in the presence of either **6** or Alexa633–phalloidin. The samples were then centrifuged. Figure 4 a shows the resulting colored pellets consisting of insoluble actin stained with the fluorescent compound and indicates the expected binding of phalloidin to F-actin, as well as that of **6** to that insoluble actin material. Thus, the vescalagin–FITC conjugate **6** directly binds F-actin.

In the same way, we quantified the amount of F-actin (pellet) relative to the amount of G-actin (supernatant) by SDS-PAGE after the centrifugation of samples treated with either **1** (100 μM), cytochalasin D (4 μM), or phalloidin (2 μM). Polymerization performed in the presence of cytochalasin D yielded a G-actin/F-actin ratio similar to that observed for the control (Figure 4 b), as expected from the ability of cytochalasin D to block actin assembly and disassembly. However, vescalagin-treated samples were characterized by a marked depletion of G-actin, similar to that observed in the case of samples treated with phalloidin. Thus, **1** promotes the actin filament state, presumably by binding to F-actin and thereby displacing the equilibrium in favor of F-actin, in a dose-dependent manner (Figure 4 c). The same effect was observed with **6** (Figure 4 d).

Analysis based on surface plasmon resonance (SPR)<sup>[13]</sup> confirmed that **1** does not bind G-actin. The vescalagin–biotin conjugate **9** was synthesized by first treating **1** with octane-1,8-dithiol to furnish the sulfhydryl thioether 1-deoxyvescalagin derivative **7** (Figure 5 a).<sup>[13]</sup> Thiol **7** was then coupled to the biotinylated maleimide linker **8**.<sup>[18a]</sup> This coupling reaction was performed in deuterated dimethyl sulfoxide (DMSO) to enable its monitoring by <sup>1</sup>H NMR spectroscopy.<sup>[18b]</sup> The reaction was complete after 7 hours at room temperature and afforded pure **9**, which was precipitated from the reaction mixture in 95% yield upon the addition of Et<sub>2</sub>O/MeOH (3:1, v/v; see the Supporting Information for details). This vescalagin–biotin conjugate was then readily immobilized in one step on streptavidin-coated sensor chips in preparation for a series of SPR analyses with G-actin and F-actin (Figure 5 b). No detectable binding occurred when a 2 μM solution of G-actin was injected onto the vescalagin-coated surface; however, the SPR response strongly increased when F-actin (prepared from the 2 μM solution of G-actin)<sup>[19]</sup> was injected. These results showed that vescalagin only binds

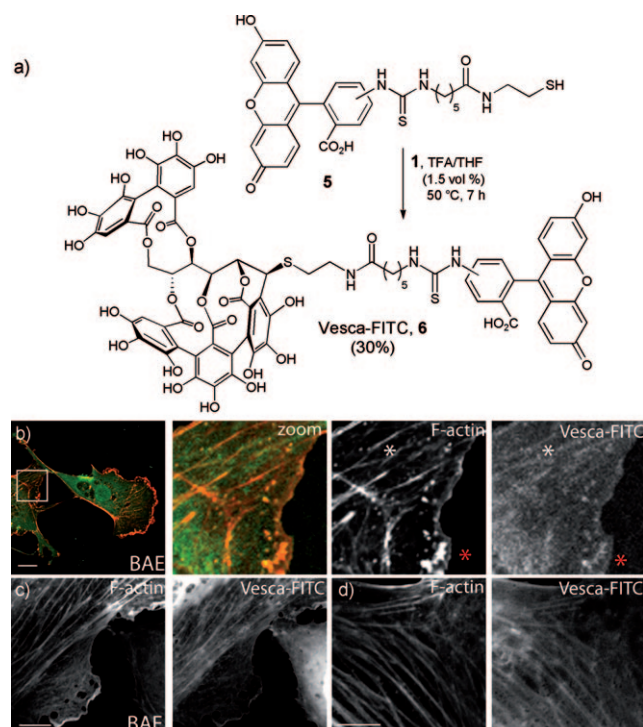


**Figure 3.** a) Preparation of the fluorescent vescalagin–FITC conjugate **6**. b) Fluorescent image of live BAE cells upon the addition of **6** (50 μM, 30 min), after fixation and staining with Alexa546–phalloidin, showing F-actin disturbance similar to that observed with **1** (scale bar: 2 μm). The zoomed view of the boxed area highlights remaining stress fibers (\*) and actin aggregates (\*). c, d) Simultaneous staining of actin filaments in lamellipodium (c) and stress fibers (d) in fixed BAE cells with Alexa546–phalloidin and **6** revealed a very similar pattern (scale bars: 7 μm). TFA = trifluoroacetic acid.

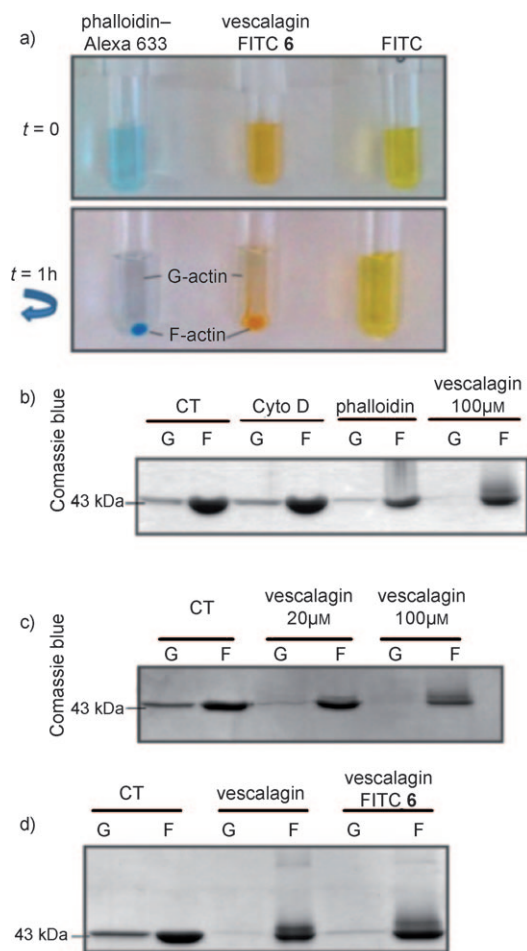


**Figure 4.** a) Actin polymerization at its steady state under both permissive and nonpermissive conditions was continued (30 min) in the presence of either Alexa633–phalloidin or **6** (vescalagin–FITC). After high-speed centrifugation, F-actin stained with Alexa633–phalloidin (blue) or with **6** (orange) was detected; however, no F-actin was detected with FITC alone. b) The fractions were examined for actin content by SDS-PAGE followed by Coomassie blue staining. Treatment with cytochalasin D yielded G-actin and F-actin in quantities similar to those obtained in the control experiment (CT), whereas samples treated with **1** or phalloidin showed a depletion of G-actin. c) This effect is dose-dependent and d) not altered by the presence of the FITC-bearing unit in **6**.

filamentous actin. The slow dissociation phase observed indicates that the vescalagin/F-actin complexes are highly stable. The absence of significant SPR responses upon the injection of 2 μM solutions of bovine serum albumin (BSA) or streptavidin further supports the specific nature of the interaction between vescalagin and F-actin.

How vescalagin affects actin polymerization was visualized by confocal microscopy. Actin polymerization was initiated with Alexa568–actin monomers in an F-actin buffer. Live imaging showed free actin filaments undergoing changes of shape on a scale of seconds; they underwent elongation in all directions. When the steady state had been reached (Figure 6a), the vescalagin–FITC conjugate **6** was added. Instantly, actin filaments were observed to agglutinate into irregular modules, which suggested that vescalagin

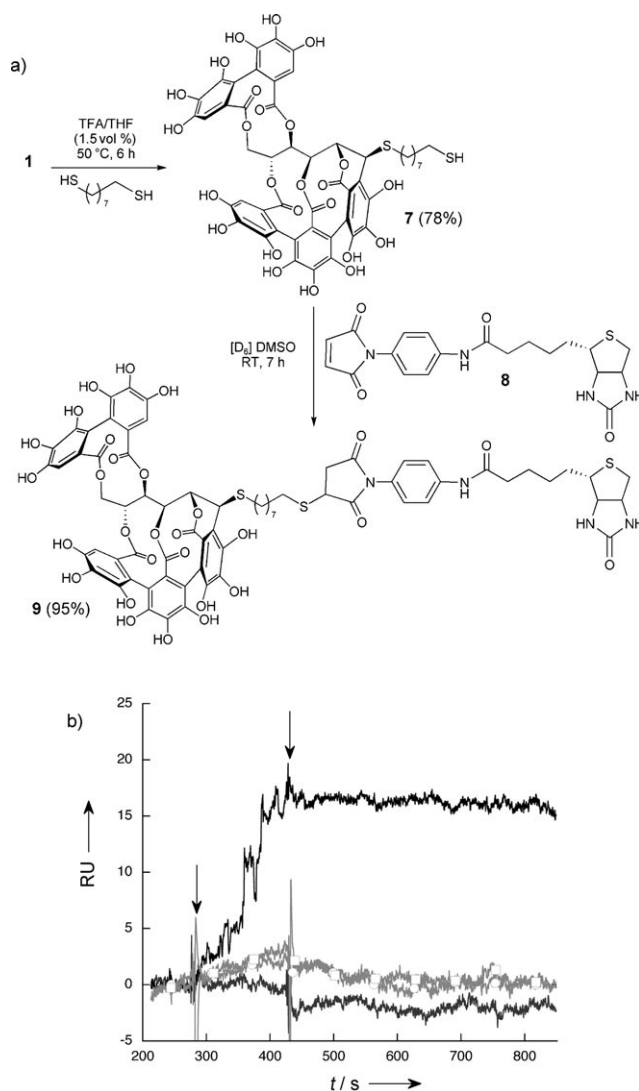


**Figure 5.** a) Synthesis of the biotinylated vescalagin conjugate **9**. b) SPR analysis of the binding of F-actin (top: black line), G-actin (bottom: dark-gray line), BSA (gray with open circles), and streptavidin (gray with open squares) to vescalagin. Compound **9** (217 RU) was immobilized on a streptavidin-coated sensor chip. Protein solutions (2 μM in running buffer) were injected across the surface at a rate of 20 μL min<sup>-1</sup> for 147 s [time elapsed between the start of injection (first arrow) and the start of the dissociation phase (second arrow)] at 25 °C. The dissociation phase was recorded for 300 s. RU = resonance units.

physically cross-linked F-actin (Figure 6b). A merged image of actin (red) and vescalagin (green) fluorescence revealed the uniform colocalization of actin aggregates with **6**.

The stabilization of filaments by phalloidin did not prevent this effect (results not shown). Therefore, the vescalagin-induced collapse of actin filaments is not mediated by actin depolymerization. When conditions under which actin remains monomeric were used (i.e., the CaCl<sub>2</sub>-containing G-actin buffer was used),<sup>[20]</sup> the distribution of the vescalagin–FITC conjugate appeared diffuse. This observation confirmed that vescalagin had no effect on G-actin (Figure 6c). Furthermore, when Ca<sup>2+</sup>-actin was converted

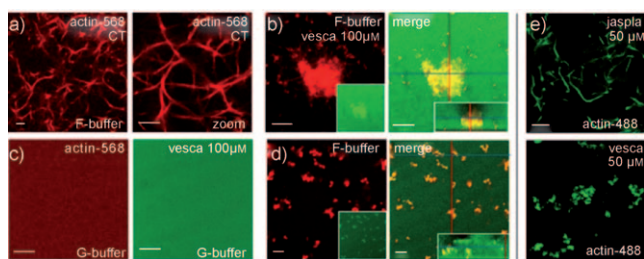


**Figure 6.** a) Live imaging of Alexa568–actin filaments grown at the steady state. b) Actin filaments had collapsed into irregular modules in less than 1 min following the addition of vescalagin–FITC (**6**; 100  $\mu\text{M}$ ). Fluorescence of Alexa568–actin (red, left; **6** can be seen in the green-channel insert) and uniform colocalization (yellow, right; the insert shows a z-cut section) of actin aggregates with **6**. c) Live imaging in the red and green channels of Alexa568–actin under conditions under which actin remains monomeric, following the addition of **6**. d) Left: actin polymerization initiated for Alexa568–actin monomers in the presence of **6** by the addition of F-actin buffer; small and sporadic clusters of aggregated F-actin (red; **6** can be seen in the green-channel insert). Right: colocalization (yellow) of actin and **6** (the insert shows a z-cut section) as observed at the onset of the experiment ( $t = 1$  min). e) Live imaging of Alexa488–actin filaments grown at the steady state after overnight exposure to jasplakinolide or vescalagin (50  $\mu\text{M}$ ). Scale bars: 5  $\mu\text{m}$ .

into  $\text{Mg}^{2+}$ –actin by the use of conditions under which actin remains monomeric (i.e., in the presence of ethylene glycol tetraacetic acid),<sup>[20]</sup> **6** was unable to aggregate actin. This result rules out any effect of the actin conformational change upon  $\text{Ca}^{2+}/\text{Mg}^{2+}$  exchange prior to polymerization.<sup>[17b]</sup> However, when **6** was added to G-actin, actin aggregation was induced upon the initiation of actin polymerization by the addition of the standard F-actin buffer. Sporadic clusters of aggregated F-actin were observed in multiple foci all over the coverslip. These clusters grew in size over time to form the aggregates shown in Figure 6d. Similar results were obtained with **1** (see Movie 7). This effect appears to be distinct from those induced by other actin-stabilizing drugs, such as jasplakinolide (Figure 6e) and phalloidin (similar results to those observed with jasplakinolide). Three-dimensional analysis of these clusters revealed a fibrillar arrangement of actin, but a random organization of the fibrils within the clusters (see Figure S8). Collectively, these findings demonstrate that **1** becomes capable of binding actin only when polymerized or undergoing polymerization into filaments. Thus, **1** presents two functions: it binds actin filaments and winds them into fibrillar aggregates.

The actin-filament-aggregation effect of **1** did not prevent actin polymerization and furthermore decreased the pool of G-actin. By extension, in cellulo, the spontaneous induction of disorganized aggregates of F-actin by **1** would be expected to circumvent regulated actin-filament elongation at filament ends and thus lead to a cellular environment in which there is insufficient polymerization-competent G-actin to maintain normal stress-fiber turnover. Alterations of cellular G-actin levels are known to affect the synthesis of actin and of other actin-regulatory proteins.<sup>[21]</sup>

In conclusion, this study demonstrates that polyphenolic C-glucosidic ellagitannins constitute another pool of natural

products with a privileged capacity for binding to actin. Vescalagin has all the requisites to be utilized as an antiactin agent in cellular biological investigations in its natural form **1** or fluorescent version **6**. Despite its high hydrophilicity,<sup>[22]</sup> vescalagin rapidly enters cells. Its dose-dependent effects on the actin cytoskeleton rely on its interaction with F-actin without any perturbation of the microtubule network. At variance with phalloidin, its effects on the actin cytoskeleton were found to be fully reversible (within 1 h of treatment and at concentrations up to 100  $\mu\text{M}$ ).

Our results are consistent with a mode of action through which the binding of vescalagin occurs along the length of the actin filament, probably at the protein–protein interface of the so-polymerized actin supramolecular association. The two analogous polyhydroxylated arene motifs (i.e., the nonahydroxyterphenoyl (NHTP) and HHDP units; see Figure 1a) are probably the key structural features that enable vescalagin to wind F-actin into fibrillar aggregates by engaging it through multiple intra- and/or intermolecular contacts. Furthermore, since phalloidin retains its actin-binding capacity for F-actin decorated with the vescalagin–FITC conjugate **6**, as well as for vescalagin-induced actin aggregates, we conclude that vescalagin and phalloidin do not bind at the same site(s). Future studies will be devoted to the elucidation of the vescalagin–actin interaction at the molecular level and to the comparative evaluation of the antiactin effects of the other C-glucosidic ellagitannins initially screened in this study. Moreover, the SPR method we developed, which uses a biotinylated vescalagin conjugate to discriminate the binding of vescalagin to F- and G-actin, confirms the utility of the technique for the observation of specific polyphenol–protein interactions.<sup>[13]</sup> The implications of these antiactin oak-derived C-glucosidic ellagitannins on human health will form the basis of our future investigations.<sup>[23]</sup>

Received: October 26, 2010

Revised: December 23, 2010

Published online: April 27, 2011

**Keywords:** actin · aggregation · natural products · polyphenols · surface plasmon resonance

- [1] a) W. Mayer, W. Gabler, A. Riester, H. Korger, *Justus Liebig's Ann. Chem.* **1967**, 707, 177–181; b) W. Mayer, H. Seitz, J. C. Jochims, K. Schauerte, G. Schilling, *Justus Liebig's Ann. Chem.* **1971**, 751, 60–68; c) G.-i. Nonaka, T. Sakai, T. Tanaka, K. Mihashi, I. Nishioka, *Chem. Pharm. Bull.* **1990**, 38, 2151–2156.
- [2] C. G. Dos Remedios, D. Chhabra, M. Kekic, I. V. Dedova, M. Tsubakihara, D. A. Berry, N. J. Nosworthy, *Physiol. Rev.* **2003**, 2, 433–473.
- [3] C. D. Nobes, A. Hall, *Cell* **1995**, 81, 53–62.
- [4] I. Spector, F. Braet, N. R. Shochet, M. R. Bubb, *Microsc. Res. Tech.* **1999**, 47, 18–37.
- [5] a) J. A. Cooper, *J. Cell Biol.* **1987**, 105, 1473–1478; b) T. Usui, *Biosci. Biotechnol. Biochem.* **2007**, 71, 300–308; c) H. Waldmann, T. S. Hu, S. Renner, S. Menninger, R. Tannert, T. Oda, H. D. Arndt, *Angew. Chem.* **2008**, 120, 6573–6577; *Angew. Chem. Int. Ed.* **2008**, 47, 6473–6477; d) R. Tannert, L. G. Milroy, B. Ellinger, T. S. Hu, H. D. Arndt, H. Waldmann, *J. Am. Chem. Soc.* **2010**, 132, 3063–3077.

- [6] a) *Chemistry and Biology of Ellagitannins: An Underestimated Class of Bioactive Plant Polyphenols* (Ed.: S. Quideau), World Scientific, Singapore, **2009**; b) S. Quideau, K. S. Feldman, *Chem. Rev.* **1996**, *96*, 475–503; c) E. Haslam, Y. Cai, *Nat. Prod. Rep.* **1994**, *11*, 41–66.
- [7] S. Quideau, M. Jourdes, D. Lefeuvre, P. Pardon, C. Saucier, P.-L. Teissedre, Y. Glories in *Recent Advances in Polyphenol Research, Vol. 2* (Eds.: C. Santos-Buelga, M. T. Escribano-Bailon, V. Lattanzio), Wiley-Blackwell, Oxford, **2010**, pp. 81–137.
- [8] a) O. Hoffmann, J. Nguemo, D. Mühlgassner, A. Liebhart, S. Quideau, *Bone* **2006**, *39*, S9–S10; b) E. K. Park, M. S. Kim, S. H. Lee, K. H. Kim, J. Y. Park, T. H. Kim, I. S. Lee, J. T. Woo, J. C. Jung, H. I. Shin, J. Y. Choi, S. Y. Kim, *Biochem. Biophys. Res. Commun.* **2004**, *325*, 1472–1480; c) T. Hatano, L. Han, S. Taniguchi, T. Okuda, Y. Kiso, T. Tanaka, T. Yoshida, *Chem. Pharm. Bull.* **1995**, *43*, 2033–2035.
- [9] a) S. Quideau, M. Jourdes, D. Lefeuvre, D. Montaudon, C. Saucier, Y. Glories, P. Pardon, P. Pourquier, *Chem. Eur. J.* **2005**, *11*, 6503–6513; b) S. Quideau, M. Jourdes, C. Saucier, Y. Glories, P. Pardon, C. Baudry, *Angew. Chem.* **2003**, *115*, 6194–6196; *Angew. Chem. Int. Ed.* **2003**, *42*, 6012–6014.
- [10] C. Varon, F. Tatin, V. Moreau, E. Van Obberghen-Schilling, S. Fernandez-Sauze, E. Reuzeau, I. Kramer, E. Génot, *Mol. Cell. Biol.* **2006**, *26*, 3582–3594.
- [11] J. F. Casella, M. D. Flanagan, S. Lin, *Nature* **1981**, *293*, 302–305.
- [12] C. Le Clainche, M.-F. Carlier, *Physiol. Rev.* **2008**, *88*, 489–513.
- [13] C. Douat-Casassus, S. Chassaing, C. Di Primo, S. Quideau, *ChemBioChem* **2009**, *10*, 2321–2324.
- [14] I. Foissner, G. O. Wasteneys, *Plant Cell Physiol.* **2007**, *48*, 585–597.
- [15] M. S. Gonçalves, *Chem. Rev.* **2009**, *109*, 190–212.
- [16] S. Soares, N. Mateus, V. de Freitas, *J. Agric. Food Chem.* **2007**, *55*, 6726–6735.
- [17] a) J. D. Pardee, J. A. Spudich, *J. Cell. Biol.* **1982**, *93*, 648–654; b) M. F. Carlier, *J. Biol. Chem.* **1991**, *266*, 1–4.
- [18] a) J. F. W. Keana, M. D. Ogan, Y. Lu, M. Beer, J. Varkey, *J. Am. Chem. Soc.* **1986**, *108*, 7957–7963; b) R. J. Pounder, M. J. Stanford, P. Brooks, S. P. Richards, A. P. Dove, *Chem. Commun.* **2008**, 5158–5159.
- [19] For a recent example of SPR analysis involving the use of a solution of F-actin, see: R. J. Barfoot, K. H. Sheikh, B. R. G. Johnson, J. Colyer, R. E. Miles, L. J. C. Jeuken, R. J. Bushby, S. D. Evans, *Langmuir* **2008**, *24*, 6827–6836.
- [20] L. Blanchoin, T. D. Pollard, *J. Biol. Chem.* **1998**, *273*, 25106–25111.
- [21] A. Sotiropoulos, D. Gineitis, J. Copeland, R. Treisman, *Cell* **1999**, *98*, 159–169.
- [22] The octan-1-ol/water partitioning coefficient  $K_{ow}$  of vescalagin is 0.1: C. M. Spencer, Y. Cai, R. Martin, T. H. Lilley, E. Haslam, *J. Chem. Soc. Perkin Trans. 2* **1990**, 651–660.
- [23] S. Quideau, E. Genot, F. Saltel, C. Douat-Casassus, D. M. Delannoy López, EP11305186, **2011**.